Proceedings of the 1992 IEEE
International Conference on Robotics and Automation
Nice, France - May 1992

Design of a Holonomic Omnidirectional Vehicle

Mark West and Haruhiko Asada

Center for Information-Driven Mechanical Systems
Department of Mechanical Engineering
Massachusetts Institute of Technology
Cambridge, MA 02139

Abstract

In this paper we introduce a new design of holonomic omnidirectional vehicle. The holonomic mechanism allows the vehicle to maneuver in an arbitrary direction from an arbitrary configuration on a plane. This significantly simplifies control problems and improves positioning accuracy. A fundamental method of obtaining omnidirectional motion with holonomic constraints with the floor, using a mechanism with spherical tires, is presented. Kinematic analysis of this mechanism gives the vehicle Jacobian relating actuator velocities to the vehicle velocity components. Analysis of lateral tire slip during vehicle rotation allows slip reduction methods. A prototype vehicle using this special mechanism and a computerized control system is designed and tested. In addition to rotation, the vehicle can perform very accurate translational motions, in two orthogonal directions, arbitrarily termed forwards *and* sideways. *Motions in these two D.O.F.'s (degrees of freedom) are decoupled from each other and are insensitive to variations in ground friction coefficient.*

1 Introduction

There is a great need for highly maneuverable vehicles to operate in industrial [1] and other [2] environments. In manufacturing industries, for instance, vehicles are required to maneuver in crowded environments and position their payload accurately at manufacturing stations. The goal of this paper is to develop a highly maneuverable, accurate vehicle that allows for holonomic, omnidirectional motion on a plane.

The importance of holonomy as a property of a vehicle is profound. As defined in standard textbooks [3], a holonomic system is a system that has the same number of independent virtual displacements as the number of generalized coordinates to locate the system. We need three generalized coordinates to locate a vehicle uniquely on a plane. Therefore, a holonomic omnidirectional vehicle is a vehicle for which all three independent planar motions, two translational and one rotational, are admissible at a non-zero velocity from arbitrary configuration.

This holonomy enables vehicles to maneuver in crowded environments, as demonstrated by the well known illustration in Figure 1. It is, however, important to note that omnidirectional motion alone is not sufficient for holonomy.

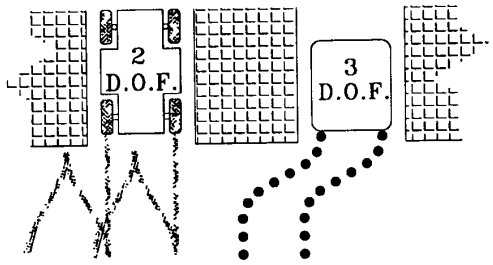

Figure 1: Typical maneuvering trajectories for 2 D.O.F. and omnidirectional vehicles.

In the past, various mechanisms have been developed that include several independently steerable wheels [4]. Of these, some are capable of continuously varying their heading through 360°, and as such may be termed omnidirectional but, strictly speaking, they are not holonomic. Most of them need to orient their wheels in the desired direction prior to the movement of the body in that direction. It is not always possible for such vehicles to negotiate a trajectory with discontinuous heading without incorperating a time delay during which the wheel orientation can be changed.

The holonomic vehicle we will discuss in this paper does not need any wheel reorientation, nor have any singular point. It is allowed to move in any direction immediately at any configuration. The vehicle can be viewed as an $XY\Theta$ positioning table with an infinite work space. Such a vehicle mechanism significantly simplifies control problems and allows for improved maneuverability and accuracy.

An existing device avoids the nonholonomic constraints on conventional wheels by attaching an array of rollers around the circumference, the axis of the rollers being skewed to the axis of the wheel [5]. Independently controlling the angular velocity of the wheel and rollers allows 2 D.O.F. motion, however, due to the mechanism complexity required to provide power to the circumferential rollers, they are usually passive [6]. Roller rotation is thus controlled by constructing a vehicle with several interacting omnidirectional wheels (usually four), providing the vehicle with a closed kinematic chain structure in the presence of sufficient floor friction. The wheels are configured such that specifying the angular velocity of all the wheels uniquely determines the angular

0-8186-2720-4/92 $3.00 ©1992 IEEE

velocity of the rollers, thus allowing 3 D.O.F. vehicle motion to be controlled [7]. The Jacobian relating wheel angular velocities to vehicle velocities is found to be fully coupled [8]. Dead reckoning and wheel slip detection algorithms have been developed [9], and several industrial applications have been found [7].

In this paper, an alternative omnidirectional vehicle is presented. The new vehicle consists of all active components and allows for completely decoupled, holonomic motions in a two-dimension work space. Accurate forward and sideways motions are achieved in the face of uneven frictional distribution of the floor.

2 A new (holonomic) omnidirectional vehicle system

2.1 A spherical tire mechanism

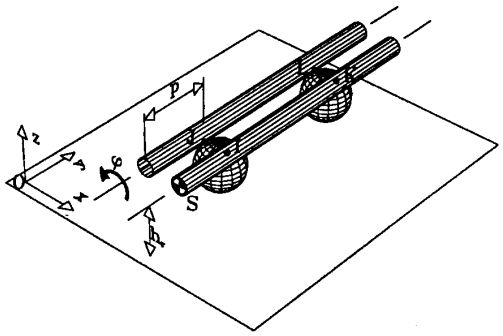

Figure 2: Omnidirectional spherical tire mechanism.

Consider spherical tires (balls) as shown in Figure 2, instead of disk shaped wheels. An inertial reference frame $O(x, y, z)$, is fixed to the ground. In order to transmit torque to the balls, as well as to guide the balls, we use a pair of rods parallel to the y axis. These rods are kept in contact with the balls at points I, J, K and L and the position reference point for the mechanism, S, is fixed at the end of one rod also as shown in Figure 2.

Let the system parameters be as follows:

R = Radius of the balls.

r = Radius of the rods.

h_r = Height of points I, J, K and L above $x - y$ plane.

Motion in the y direction is achieved by moving the balls along the length of the rods. Sliding is prohibited and thus the balls rotate about axes parallel to the x direction. Motion in the x direction is achieved by rotating the rods about their axes which in turn rotates the balls about axes parallel to the y direction. The system has two admissible independent virtual displacements (D.O.F.'s) δ_x and δ_y.

A complete set of generalized coordinates for the system is as follows:

$x\ (y) = x\ (y)$ coordinate of mechanism reference point, S.

ϕ = angular position of rods about axes.

p = distance between points S and I.

2.2 Kinematics of mechanism

Now, assuming no slippage between the balls and the ground and the balls and the rods, we find the relationship between (x, y) and (ϕ, p).

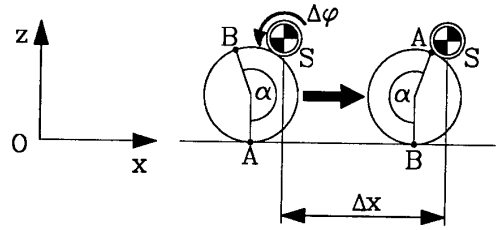

Figure 3a: Section through vehicle in $x - z$ plane before and after motion Δx.

To consider motion in the x direction let us examine a section in the $x - z$ plane as shown in Figure 3a. Let us rotate the rods through angle $\Delta\phi$. The resultant rotation of the ball about an axis parallel to the y direction will be through angle α. The no slip constraint between ball and rod yields:

$$r\Delta\phi = R\alpha \tag{1}$$

For no slip between the ball and the ground the displacement of point S in the x direction is given by:

$$\Delta x = R\alpha = r\Delta\phi \tag{2}$$

Note that the diameter of the ball is irrelevant.

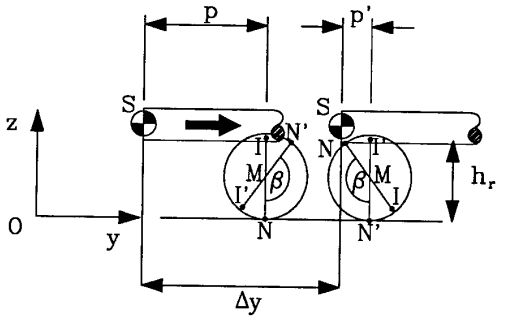

Figure 3b: Section through vehicle in $y - z$ plane before and after motion Δy.

Similarly to consider the motion in the y direction let us examine a section in the $y - z$ plane showing one ball as in Figure 3b. Let the center point of the ball be M and the points of contact with the ground and rod be N and I respectively. Let the ball rotate through angle β about an axis parallel to the x direction. The new point of contact between the ball and the ground is N' while the new point of contact between the ball and the rod is I'. The distance between I and S, originally p, becomes the distance between I' and S, namely p'. The change in the y coordinate of S is Δy where:

$$\Delta y = (h_r - R)\beta + R\beta = h_r\beta \tag{3}$$

Also:

$$\Delta p = p' - p = -(h_r - R)\beta \tag{4}$$

Combining (3) and (4):

$$\Delta y = -\frac{h_r}{h_r - R}\Delta p \tag{5}$$

Note from equations (2) and (5) that the two variables Δp and $\Delta\phi$ are a complete and independent set of generalized coordinates to locate the vehicle position, $S(x, y)$. Both geometric constraints (2) and (5) are holonomic as they are expressions relating generalized coordinates [3].[1]

Choosing an appropriate location for the origin of the inertial reference frame we can combine equations (2) and (5) to give:

$$\begin{bmatrix} x \\ y \end{bmatrix} = \begin{bmatrix} r & 0 \\ 0 & -\frac{h_r}{h_r - R} \end{bmatrix} \begin{bmatrix} \phi \\ p \end{bmatrix} \tag{6}$$

An arbitrary linear velocity $v = [\dot{x}, \dot{y}]^T$ can be generated; the vehicle can be moved in an arbitrary direction within the horizontal plane.

2.3 Basic construction

We construct a vehicle using two of the 2 D.O.F. holonomic spherical tire mechanisms shown in Figure 2. These units will be referred to as 'tracks' here-on-in. The two tracks are a fixed relative to each other in the vehicle chassis as shown in Figure 4.

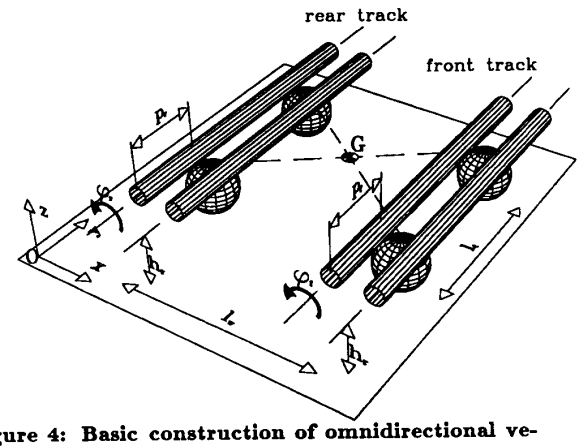

Figure 4: Basic construction of omnidirectional vehicle.

[1]It should be noted at this point that we do not describe the orientation of the balls by the generalized coordinates. If this had been the case, the system would not be holonomic as there would be four independent generalized coordinates, (x, y and two angles defining ball orientation),but only 2 D.O.F's. The physical interpretation is that vehicle position (x, y) does not uniquely define the ball orientation. However, as we are not interested in ball orientation, but just the vehicle position, this system can be described as holonomic.

We choose a new position reference point $G(x_G, y_G)$ such that G is fixed in the center of the vehicle. The existing mechanism parameter definitions remain. We define the new parameters as follows:

l_t = tred. Length of track over which balls contact ground.

l_w = wheelbase. Distance between track centerlines.

We redefine the mechanism variables as follows:

ϕ_f (ϕ_r) = angular rotation of rods in front (rear) track.

p_f (p_r) = distance from end of rod to point of contact with first ball in front (rear) track.

Since we assume no slippage:

$$\phi_f = \phi_r = \phi \tag{7}$$

A crawler mechanism is employed which allows for infinite motion in the direction parallel to the rods by recirculating the balls to ensure that there are always balls between the rods and the ground. The mechanism comprises a belt which moves the balls along the rods thus changing p_f and p_r. The belt in each track is driven through a sprocket and the angular position of the sprockets in the front and rear tracks are not constrained to be equal. Thus we define:

r_s = pitch radius of sprockets.

ψ_f (ψ_r) = angular position of sprockets in front (rear) track.

Hence:

$$p_f = r_s\psi_f \qquad p_r = r_s\psi_r \tag{8}$$

Independently driving ψ_f and ψ_r allows a third D.O.F., vehicle rotation, and accordingly we define a third vehicle generalized coordinate in addition to the position of $G(x_G, y_G)$:

θ = angle between rod centerlines and y axis measured in a positive sense about the z axis.

Now if $v_x = \dot{x_G}$, $v_y = \dot{y_G}$ and $\omega = \dot{\theta}$ then:

$$\begin{bmatrix} v_x \\ v_y \\ \omega \end{bmatrix} = \begin{bmatrix} \quad \\ \mathbf{J} \\ \quad \end{bmatrix} \begin{bmatrix} \dot{\phi} \\ \dot{\psi_f} \\ \dot{\psi_r} \end{bmatrix} \tag{9}$$

We will now derive $\mathbf{J}$ for the case when $\theta = 0$. First we obtain the equation for motion in the x direction by differentiating equation (6):

$$v_x = r\dot{\phi} \tag{10}$$

Next, in order to find the equation for motion in the y direction, let us define:

y_f (y_r) = y coordinate of center of front (rear) track.

From equations (6) and (8):

$$\dot{y_f} = -\frac{h_r}{h_r - R}\dot{p_f} = -\frac{h_r}{h_r - R}r_s\dot{\psi_f} \tag{11}$$

$$\dot{y_r} = -\frac{h_r}{h_r - R}\dot{p_r} = -\frac{h_r}{h_r - R}r_s\dot{\psi_r} \tag{12}$$

Now the front and rear tracks are fixed to each other and therefore $\dot{y}$ will vary linearly as we move along the wheelbase

of the vehicle. G is in the center of the vehicle.
Therefore:

$$v_y = \dot{y}_G = \frac{1}{2}(\dot{y}_f + \dot{y}_r) = -\frac{r_s h_r}{2(h_r - R)}(\dot{\psi}_f + \dot{\psi}_r) \qquad (13)$$

Finally, consider virtual displacements δy_f and δy_r with $\delta y_f \neq \delta y_r$ resulting in virtual vehicle rotation, as shown in Figure 5. Some tire slip will occur during vehicle rotation as analyzed in the next section. However, here we assume that the tires at the center of the track do not slip. This gives us the magnitude of the virtual rotation:

$$\delta\theta \approx \frac{\delta y_f - \delta y_r}{l_w} \qquad (14)$$

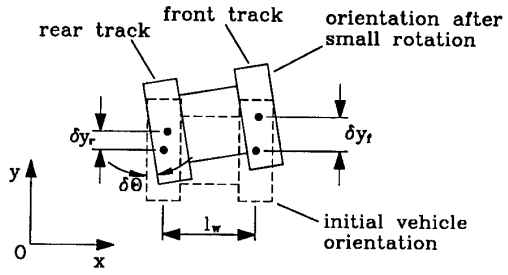

Figure 5: Virtual displacements in track position δy_f and δy_r resulting in virtual rotation $\delta\theta$.

Combining equations (11), (12) and (14):

$$\omega = \dot{\theta} = \frac{\dot{y}_f - \dot{y}_r}{l_w} = -\frac{r_s h_r}{l_w(h_r - R)}(\dot{\psi}_f - \dot{\psi}_r) \qquad (15)$$

Equations (10), (13) and (15) give us the Jacobian:

$$\begin{bmatrix} v_x \\ v_y \\ \omega \end{bmatrix} = \begin{bmatrix} r & 0 & 0 \\ 0 & -\frac{r_s h_r}{2(h_r - R)} & -\frac{r_s h_r}{2(h_r - R)} \\ 0 & -\frac{r_s h_r}{l_w(h_r - R)} & \frac{r_s h_r}{l_w(h_r - R)} \end{bmatrix} \begin{bmatrix} \dot{\phi} \\ \dot{\psi}_f \\ \dot{\psi}_r \end{bmatrix} \qquad (16)$$

Equations (10), (13) and (15) are holonomic constraints as each is integratable into an expression relating generalized coordinates only. Therefore the system is holonomic as all its motion constraints are. Indeed it has a set of three complete and independent generalized coordinates, (x_G, y_G, θ), and 3 D.O.F's.

However note that (θ, ψ_f, ψ_r) do not uniquely define (x_G, y_G). Rather variations of (θ, ψ_f, ψ_r) with time must be known as the effect of infinitesimal changes $(\delta\theta, \delta\psi_f, \delta\psi_r)$ on (x_G, y_G) depends on the orientation θ. In contrast θ can be calculated at any instant in time from the absolute values ψ_f and ψ_r.

3 Tire slip analysis

In this section we will analyze tire slip during vehicle rotation and obtain a method for alleviating the tire slip problem. To achieve translational motions all the balls move with equal angular velocity vectors, $(\dot{\psi}_f = \dot{\psi}_r)$, however to avoid slip during vehicle rotation each ball requires a different angular velocity vector. This cannot be achieved with the mechanism described by Figure 4 as all balls in the same track are constrained to move with the same angular velocity vector, and hence some tire slip will occur during vehicle rotation. The magnitude of this slippage will first be evaluated. Let us define the parameter to be minimized, the slip ratio γ, given by:

$$\gamma = \frac{|\mathbf{v_s}|}{\omega} \qquad (17)$$

where:
$\mathbf{v_s}$ = maximum slip velocity between any tire and ground.
ω = angular velocity of vehicle.

Let the vehicle coordinates $(x, y, \theta) = (0,0,0)$ such that G and O coincide. A desired arbitrary motion, $[v_x, v_y, \omega]^T$, can be represented by a rotation at angular velocity ω about an instantaneous center, $E(x_E, y_E)$, as shown in Figure 6.

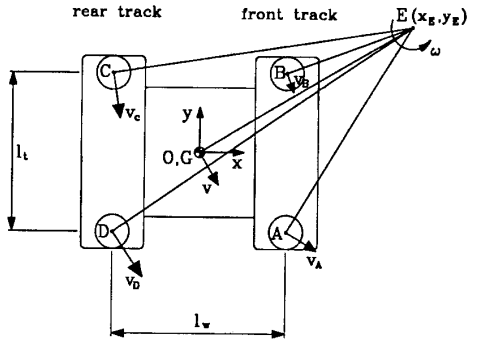

Figure 6: Arbitrary vehicle velocity represented by rotation ω about point E.

Let A, B, C and D be the corner points of the vehicle. The maximum slip velocity must occur at A, B, C or D. Let v_{Ax} and v_{Ay} be x,y components of velocity of point A if desired rotation about E occurs. Let v'_{Ax} and v'_{Ay} be x,y components of velocity at which the tire at point A is driven, as specified by the inverse of Jacobian (16), to rotate about E.

The difference between the actual velocity of a point and the velocity at which the tire at that point is driven is the slip velocity at that point.

To achieve the desired rotation about E, the required translational motion of point G, $\mathbf{v}$, is:

$$\mathbf{v} = \omega \times \overline{EG} \qquad (18)$$

where: $\overline{EG} = [-x_E, -y_E]^T$
v_x and v_y are obtained directly by substituting $[-x_E, -y_E]^T$ to (18).
hence:

$$v_x = y_E\omega \qquad v_y = -x_E\omega \qquad (19)$$

Substituting (19) into the inverse of Jacobian (16):

$$\begin{bmatrix} \dot{\phi} \\ \dot{\psi_f} \\ \dot{\psi_r} \end{bmatrix} = \omega \begin{bmatrix} \frac{1}{r} & 0 & 0 \\ 0 & -\frac{(h_r-R)}{r_s h_r} & -\frac{l_w(h_r-R)}{2r_s h_r} \\ 0 & -\frac{(h_r-R)}{r_s h_r} & \frac{l_w(h_r-R)}{2r_s h_r} \end{bmatrix} \begin{bmatrix} y_B \\ -x_B \\ 1 \end{bmatrix} \quad (20)$$

which determines the angular velocities of the rods, $\dot{\phi}$, and of the drive sprockets in the front and rear tracks, $\dot{\psi_f}$ and $\dot{\psi_r}$ respectively.

From equations (10) and (20) it is seen that points A,B,C and D are all driven in the x direction at speed:

$$v'_{Ax} = v'_{Bx} = v'_{Cx} = v'_{Dx} = \dot{\phi} r = \omega y_B \quad (21)$$

Combining equations (11) and (20) gives the speed at which points A and B are driven in the y direction.

$$v'_{Ay} = v'_{By} = -\frac{h_r}{h_r - R} r_s \omega \frac{(h_r - R)(x_B - \frac{l_w}{2})}{r_s h_r} = -\omega(x_B - \frac{l_w}{2}) \quad (22)$$

Combining equations (12) and (20) gives the speed at which points A and B are driven in the y direction.

$$v'_{Cy} = v'_{Dy} = -\frac{h_r}{h_r - R} r_s \omega \frac{(h_r - R)(x_B + \frac{l_w}{2})}{r_s h_r} = -\omega(x_B + \frac{l_w}{2}) \quad (23)$$

Now to achieve the desired angular velocity about E the actual velocity of point A is given by:

$$\mathbf{v_A} = \omega \times \overline{EA} \quad (24)$$

where $$\overline{EA} = [-x_B + \tfrac{l_w}{2}, -y_B - \tfrac{l_t}{2}]^T$$

hence

$$\mathbf{v_A} = \left[\omega(y_B + \frac{l_t}{2}), -\omega(x_B - \frac{l_w}{2})\right]^T \quad (25)$$

Similarly we can obtain velocities at points B, C and D.

It is seen that $v'_{Ay} = v'_{By} = v_{Ay} = v_{By}$ and $v'_{Cy} = v'_{Dy} = v_{Cy} = v_{Dy}$ and therefore there is no slip in the y direction. However:

$$v'_{Ax} - v_{Ax} = \omega y_B - \omega(y_B + \frac{l_t}{2}) = -\omega \frac{l_t}{2} \quad (26)$$

Consequently slip velocity at A is $-\omega \frac{l_t}{2}$ in x direction. Similar results are obtained for points B, C and D.

Equation (26) shows that maximum slip occurs with equal magnitude and in opposite directions at opposite ends of each track. Hence there is no slip at the center of each track. This is the assumption which was made in the derivation of equation (14) and consequently the Jacobian. Equation (26) also show that the magnitude of slip is linearly dependent on the position along the length of the track and that it is independent of the wheelbase, l_w, or the position of E. If the center of mass is at the center of the vehicle, G, and the coefficient of friction between the tires and the floor is constant, then by symmetry vehicle rotation will indeed be about G. Hence there will be no slip at the center of each track and the assumption is valid. Driving the rods and sprockets as specified by the Jacobian will result in the desired motion, rotation about E.

Tire slip occurs in the x direction only and slip ratio is independent of the wheelbase of the vehicle,l_w and the position of E:

$$\gamma = \frac{|\mathbf{v_S}|}{\omega} = \frac{l_t}{2} \quad (27)$$

A desirable way to minimize the slippage during rotation would be to produce rods which could be driven with an angular velocity gradient along their length. This would entail a very complex mechanism. A more feasible method of limiting the slip to an acceptable level is simply to limit the length l_t.

4 Prototyping

4.1 Mechanical design

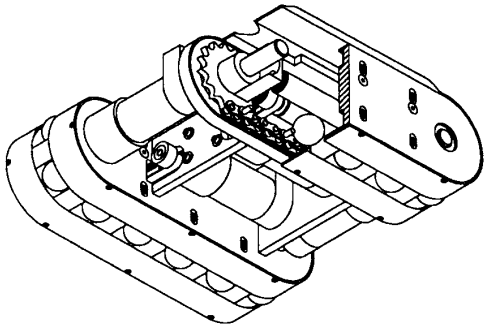

Figure 7: View of underside of vehicle, cut away to show mechanism.

We have built a prototype vehicle implementing the new principle, as illustrated in Figure 7. The overall dimensions of the vehicle are 8.5" × 8.5" and construction is essentially from aluminum.

The chassis of the vehicle comprises two parallel track like structures, rigidly fixed to each other. Inside each track the chassis holds two rubber coated steel rods. Thrust and radial bearings at each end of these rods support the vehicle with minimal friction. Rubber balls in turn support these rods from the ground. The rods are rotated by brushed permanent magnet d.c. motors, through a gearbox and a toothed belt. Although $\phi_f = \phi_r = \phi$ it was decided that two motors would be used, (one for each track), to independently drive ϕ_f and ϕ_r. This allows control of power distribution and may be useful in negotiating adverse terrain.

The ball recirculating mechanism consists of two roller chains, one on either side of the track, with rollers spanning the two at regular intervals. The balls sit between these rollers, with minimal clearance to minimize backlash. The chains are driven through gearboxes and sprockets using brushed permanent magnet d.c. motors, one for each track. As the chains move, the rollers push the balls along the length of the rods, changing p_f and p_r, thus causing vehicle motion. The rollers push the balls on their 'equators' such that simultaneous rotation of the rods will not cause

slippage but rotation about the contact point. In reality the contact will be over a small area, generating friction that would cause slight coupling between the two translational D.O.F.'s. The use of Teflon for the rollers minimizes this effect.

4.2 Control system

We aim to control the position and orientation of the vehicle in real time. A control system has been implemented on an I.B.M. PS 2, based on the kinematics of the vehicle and a dead reckoning algorithm [9], as shown in Figure 8. We plan to use dead reckoning for long distance navigation as this provides the flexibility of having all sensors on-board.

A trajectory is input in real time in the form of a position reference which is recursively updated on each control period. This information currently comes from a trajectory planner into which a human operator inputs the new desired vehicle coordinates, $G,(x,y,\theta)$. A trajectory is planned which varies all D.O.F's simultaneously taking the most direct route. The vehicle velocity is ramped from zero to a specified velocity, the vehicle then travels at this constant velocity for some time then the velocity ramps down to zero at the desired location. Alternatively, trajectories could be pre-programmed, generated automatically [10], [11], or input in real time using a 3 D.O.F. joystick.

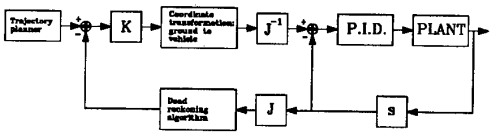

Figure 8: Block diagram for control system implemented for prototype vehicle.

The position reference is input to the trajectory control loop and compared to the calculated current vehicle position. A gain **K** applied to the position error provides a corrective velocity vector command relative to the inertial reference frame $O,(x,y,\theta)$. A coordinate transformation matrix **T** transforms the velocity command to a frame of reference fixed on the vehicle, to account for the orientation θ. This allows the transformed velocity command to be entered into the inverse of the Jacobian from equation (16) which was derived for the case $\theta = 0$.

$$\mathbf{T} = \begin{bmatrix} \cos\theta & \sin\theta & 0 \\ -\sin\theta & \cos\theta & 0 \\ 0 & 0 & 1 \end{bmatrix} \tag{28}$$

The inverse Jacobian gives the motor velocities required for the desired motion and these are given as reference inputs to the local motor velocity control loop. Encoders placed on each motor shaft measure the angular position and the average shaft velocity in each sampling period is determined by dividing the change in shaft position by the sampling period. These motor velocities are compared to the velocity reference input from the inverse Jacobian. A P.I.D. operation on the difference assures that the actual motor velocities track the required velocities as close as possible.

The motor velocities are also fed back to the trajectory control loop. The Jacobian from equation (16) gives the actual vehicle velocity relative to a frame of reference fixed on the vehicle from the motor velocities. The dead reckoning algorithm [9], is then used to update the calculated vehicle position as follows:

Let t_1 be time at beginning of sampling/control period.
Let t_2 be time at end of sampling/control period.

At any time θ can be calculated from equation (15) integrated. Thus:

$$\begin{aligned} \theta_{t_1} &= \frac{r_s h_r}{l_w(h_r - R)}(\psi_f - \psi_r)_{t_1} \\ \theta_{t_2} &= \frac{r_s h_r}{l_w(h_r - R)}(\psi_f - \psi_r)_{t_2} \end{aligned} \tag{29}$$

Now:

$$\begin{bmatrix} x \\ y \end{bmatrix}_{t_2} = \begin{bmatrix} x \\ y \end{bmatrix}_{t_1} + \frac{(t_2 - t_1)}{2}(\mathbf{T}_{\mathbf{t_2}}^{-1}\begin{bmatrix} \dot{x} \\ \dot{y} \end{bmatrix}_{t_2} + \mathbf{T}_{\mathbf{t_1}}^{-1}\begin{bmatrix} \dot{x} \\ \dot{y} \end{bmatrix}_{t_1})$$

Where:
$\mathbf{T}_{\mathbf{t_1}}^{-1}$ ($\mathbf{T}_{\mathbf{t_2}}^{-1}$) = coordinate transformation matrix from vehicle reference frame to ground reference frame with orientation θ_{t_1} (θ_{t_2}) at time t_1 (t_2).

5 Testing

To date the performance of the vehicle and its control system have been tested by commanding motion to a new position and accurately measuring the displacement of the vehicle using vernier calipers. It has been found that translational motions are currently accurate to within 1% of the commanded displacement and that no coupling between the forward-backward motion and sideways motion is detectable. This experiment has been repeated on various surfaces, from glass to rubber, and similar translational accuracies have been found despite these variations in the floor friction.

An absolute position sensor is currently being developed to allow the position of the vehicle to be precisely sampled during motion, enabling the tracking accuracy to be assessed. In the absence of such a sensor, data to illustrate the capabilities of the vehicle was collected using video. The motion of the vehicle was recorded using a camera oriented vertically, above the floor plane. Several maneuvers were then instructed to the vehicle. Using a V.C.R. and television the position and orientation of the vehicle at 10 frame (0.33 second) intervals was traced onto a transparency, a reduction

of which is shown in Figure 10.

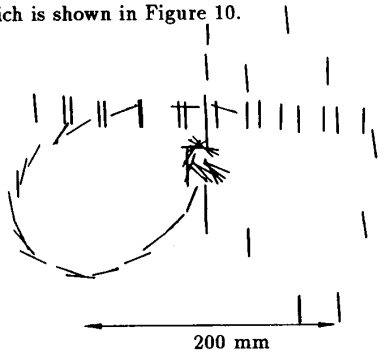

Figure 10: Position and orientation of vehicle at 0.33 second intervals during various maneuvers.

The ' | ' points represent vehicle position and orientation on the floor plane, each end of the symbol being fixed in the vehicle. As can be seen, the vehicle was first driven forwards and backwards, then from side to side, demonstrating the translational D.O.F.'s. Their decoupling is exhibited by driving these D.O.F.'s simultaneously, resulting in the diagonal trajectories forming a diamond. Rotation about the center of the symbol is then demonstrated with some apparent error in locating the center of rotation in addition to some drift of its position. Finally a circular trajectory was commanded and here it is seen that considerable errors exist caused by a significant drift of the center of rotation.

6 Conclusion

We have presented a method of achieving 3 D.O.F. holonomic motion on a plane. A vehicle mechanism using this method of locomotion has been designed and kinematic analysis has lead to holonomic equations of motion and the vehicle Jacobian. The two translational motions are seen to be decoupled from each other and no slip occurs during translation, thus enabling accurate position control in these two D.O.F.'s. The third D.O.F., rotation, results in tire slip in a direction perpendicular to the 'tracks' of the vehicle. The magnitude of this slip depends only on the angular velocity of the vehicle and the length of the tracks.

A prototype vehicle has been constructed using this design of mechanism and a control system has been implemented based on the kinematics of the vehicle and a dead reckoning algorithm. Testing of the vehicle and its controls has revealed that holonomic omnidirectional motion is exhibited and we are able to simultaneously and arbitrarily control all three degrees of freedom. The two translational motions are found to have a positional accuracy of within 1% and are not affected by each other or variations in floor friction. Vehicle rotation is found to be less accurate as the center of rotation can move from the center of the vehicle, G, if friction varies.

Future work will be aimed at maximizing tracking accuracy by improving hardware and developing a more sophisticated control system including a dynamic model of the vehicle and backlash compensation. A position feedback system will be developed for highly accurate positioning relative to interacting machinery however global absolute position sensors will be avoided as they reduce the flexibility of the system. Rather, dead reckoning, with all sensors on board, will be used for long distance navigation and the accuracy of this method must be maximized.

The device explained above can be considered a 3 D.O.F. manipulator with unlimited workspace. Additional D.O.F.'s may be incorporated by mounting a further manipulation device on the vehicle. To mention one potential application, we feel that the ability to accurately and easily control the position of objects in many D.O.F's with a workspace encompassing a whole factory offers significant advantages to manufacturing industry. In particular this allows the removal of fixed material flow paths and dedicated robotic devices as we move toward more flexible manufacturing environments.

Acknowledgements

This work was partially supported by the Leaders for Manufacturing Program, M.I.T.

We would like to thank Mr. Akihira Nishikawa for his contribution in the implementation of the vehicle control system.

References

[1] R. Dillman, "Mobile Robots in Industrial Environment", *Int. Symposium on Industrial Robots*, April 1988.

[2] G. Berger, J. M. Valade, G. Fraize, "Presentation of the Eureka Project: Advanced Mobile Robots for Public Safety Applications", MATRA, France, 1986.

[3] Crandall, Karnopp, Kurtz, Pridmore-Brown, "*Dynamics of Mechanical and Electromechanical Systems*", Krieger Publishing, 1985.

[4] J. C. Alexander, J. H. Maddocks, "On the Kinematics of Wheeled Mobile Robots", *Int. Journal of Robotics Research*, October 1989.

[5] B. E. Ilon, "Wheels for a Course Stable Selfpropelling Vehicle Movable in any Desired Direction on the Ground or Some Other Base", U.S. Patent No. 3,876,255, 1975.

[6] J. M. Holland, "*Basic Robotics Concepts*", Howard W. Sams & C0., Indianapolis, IN, 1983.

[7] S. Jonsson, "New A.G.V. with Revolutionary Movement," *3rd Int. Conference on Automated Materials Handling*, March 1986.

[8] P. F. Muir, C. P. Neuman, "Kinematic Modeling of Wheeled Mobile Robots", *Journal of Robotic Systems*, 1987.

[9] P. F. Muir, C. P. Neuman, "Kinematic Modeling for Feedback Control of an Omnidirectional Wheeled Mobile Robot", Dept. Electrical and Computer Engineering, The Robotics Institute, C.M.U., 1987.

[10] M. Sekiguchi, S. Nagata, K. Asakawa, "Behavior Control for a Mobile Robot by Multi-Hierarchical Neural Network", A. I. Laboratory, Fujitsu, Kawasaki, Japan, 1989.

[11] Y. Nakano *et. al.*, "A Concept for an Autonomous Mobile Robot and a Prototype Model", *Int. Conference on Advanced Robotics*, September 1985.